

Green Chemistry

Accepted Manuscript



This article can be cited before page numbers have been issued, to do this please use: H. Tang, N. Li, G. Li, A. Wang, C. Yu, G. Xu, X. Wang and T. Zhang, *Green Chem.*, 2019, DOI: 10.1039/C9GC00571D.



This is an Accepted Manuscript, which has been through the Royal Society of Chemistry peer review process and has been accepted for publication.

Accepted Manuscripts are published online shortly after acceptance, before technical editing, formatting and proof reading. Using this free service, authors can make their results available to the community, in citable form, before we publish the edited article. We will replace this Accepted Manuscript with the edited and formatted Advance Article as soon as it is available.

You can find more information about Accepted Manuscripts in the [author guidelines](#).

Please note that technical editing may introduce minor changes to the text and/or graphics, which may alter content. The journal's standard [Terms & Conditions](#) and the ethical guidelines, outlined in our [author and reviewer resource centre](#), still apply. In no event shall the Royal Society of Chemistry be held responsible for any errors or omissions in this Accepted Manuscript or any consequences arising from the use of any information it contains.

ARTICLE

Synthesis of gasoline and jet fuel range cycloalkanes and aromatics with poly(ethyleneterephthalate) wastesHao Tang,^{a,b} Ning Li,^{a,c*} Guangyi Li,^a Aiqin Wang,^a Yu Cong,^a Guoliang Xu,^a Xiaodong Wang^a and Tao Zhang^{a,b}Received 00th January 20xx,
Accepted 00th January 20xx

DOI: 10.1039/x0xx00000x

For the first time, gasoline and jet fuel range C₇-C₈ cycloalkanes and aromatics were selectively synthesized by the alcoholysis of poly(ethyleneterephthalate) (PET) waste, followed by the solvent-free hydrogenation and hydrodeoxygenation (HDO). It was found that methanol is highly reactive for the alcoholysis of PET waste. In the absence of any catalyst, high yield of dimethyl terephthalate (97.3%) was achieved under mild conditions (473 K, 3.5 h). The dimethyl terephthalate exists as solid and can be automatically separated from methanol with the decreasing of temperature. Subsequently, dimethyl terephthalate was liquefied to dimethyl cyclohexane-1,4-dicarboxylate by the hydrogenation over noble metal catalysts. Among the investigated catalysts, Pt/C exhibited the highest activity. Finally, the dimethyl cyclohexane-1,4-dicarboxylate as obtained was further hydrodeoxygenated to C₇-C₈ cycloalkanes and aromatics that can be used as gasoline or additives to improve the densities (or volumetric heat value) and sealabilities of current bio-jet fuels. Bimetallic Ru-Cu/SiO₂ was found to be a promising HDO catalyst. According to the characterization results, the excellent HDO performance of Ru-Cu/SiO₂ can be explained by the formation of smaller Ru-Cu alloy particles during the catalyst preparation. In real application, dimethyl cyclohexane-1,4-dicarboxylate can also be simultaneously hydrodeoxygenated with biomass derived oxygenates to produce the jet fuel with proper contents of cycloalkanes and aromatics.

Introduction

Energy and environment are two of the most concerned issues we are facing nowadays. With the declining of fossil energy, the exploration of new organic carbon resource as substitute for the production of fuels¹ and chemicals² has become a research hotspot. As one of the options, plastics have been produced in industrial scale with the feedstocks mainly derived from petroleum. The global annual production of plastics was estimated to reach 334.83 million tons by 2020.³ These materials have been widely used in many areas (such as packaging, textile industry, construction, etc.). Due to the lack of efficient technology, only a small part (~14%) of plastics is recycled.^{4, 5} Most of plastics are discarded or directly burnt after the usage, which brings a lot of environmental problems. From the point views of energy conservation and environmental protection, it is imperative to develop new technologies for the utilization of the waste plastics as the feedstocks for the production of great demanded fuels and bulk chemicals.⁶

Poly(ethylene terephthalate) (PET) is a widely used plastic. Due to its excellent mechanical and thermal properties, PET is produced in great scale (> 50 million tons per year).⁵ Because PET is highly resistant to biological degradation, the recycling of PET wastes by chemical methods has drawn tremendous attention in recent years.^{7, 8} So far, most of reported processes were concentrated on the degradation of PET to terephthalic acid⁹ or its esters (such as bis(hydroxyalkyl) terephthalate (BHET))¹⁰ and the further hydrogenation of these compounds to 1,4-cyclohexanedicarboxylates¹¹ or 1,4-cyclohexanedimethanol (1,4-CHDM).¹² Cyclic hydrocarbons (including cycloalkanes and aromatics) are important components of gasoline and jet fuel (two most demanded transportation fuels). Compared with chain alkanes, cyclic hydrocarbons have relatively higher octane-numbers, densities (or volumetric heat values) and sealabilities. Taking into consideration of the special chemical structure of PET (see Scheme 1), we think that it can be used as a potential feedstock for the production of gasoline and jet fuel range cyclic hydrocarbons. To the best of our knowledge, there is no report about this.

In this work, gasoline and jet fuel range C₇-C₈ cycloalkanes and aromatics were first synthesized by the methanolysis of PET waste, followed by the hydrogenation of dimethyl terephthalate (DMT) to dimethyl cyclohexane-1,4-dicarboxylate (DMCD) and the subsequent hydrodeoxygenation (HDO) of DMCD under solvent-free conditions. The strategy for this process was illustrated in

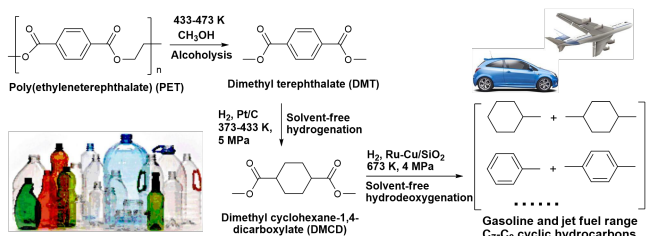
^a Dalian Institute of Chemical Physics, Chinese Academy of Sciences, No. 457 Zhongshan Road, Dalian 116023, China. E-mail: lining@dicp.ac.cn

^b University of Chinese Academy of Sciences, 19 A Yuquan Road, Shijingshan District, Beijing 100049, China.

Dalian National Laboratory for Clean Energy, No. 457 Zhongshan Road, Dalian 116023, China.

Electronic Supplementary Information (ESI) available: [Characterization of M/C catalysts. GC chromatograms, photos, mass spectrograms of the hydrogenation and hydrodeoxygenation products]. See DOI: 10.1039/x0xx00000x

Scheme 1. As we know, most of current bio-jet fuels are composed of chain alkanes. Compared with conventional jet fuel (a mixture of chain alkanes, cycloalkanes and aromatics), these bio-jet fuels have lower densities (or volumetric heat values) and sealabilities. To solve this problem, we also explored the simultaneous HDO of DMCD and some representative bio-jet fuel precursors to get jet fuels which have proper amounts of cycloalkane and aromatics.



Scheme 1. Strategy for the synthesis of gasoline and jet fuel range C_7 - C_8 cyclic hydrocarbons with PET wastes.

Experimental

Materials and methods

In this work, the drinking water bottle of Nongfu Spring® was used as a representative for the waste PET. Before being used in the alcoholysis test, the bottle was cut into 2 mm × 3 mm species with scissors. Activated carbon loaded noble metal (denoted as M/C, M = Pt, Ru or Pd) catalysts used in the solvent-free hydrogenation of DMT to DMCD were purchased from Aladdin company. Pt, Ru and Pd were chose as active metals because their higher activity of the hydrogenation of aromatic ring or ester group.¹³ According to the information from the supplier, the metal contents in the catalysts were 5wt%. The specific BET surface areas, average particle sizes and metal dispersions of the investigated M/C catalysts were illustrated in Table S1 in supporting information. The Ru/SiO₂ and Cu/SiO₂ catalysts used in the solvent-free HDO of DMCD were prepared by the incipient wetness impregnation of SiO₂ (QingdaoOcean Chemical Ltd.) with the aqueous solutions of RuCl₃·3H₂O and Cu(NO₃)₂·3H₂O, respectively. For comparison, the theoretical metal contents in the catalysts were fixed as 5wt%. After impregnation, the samples were kept at room temperature for 8 h, dried at 393 K overnight and calcined in air at 773 K for 4 h. Analogously, the bimetallic Ru-Cu/SiO₂ catalyst was prepared by the incipient wetness co-impregnation of SiO₂ with the solution of RuCl₃·3H₂O and Cu(NO₃)₂·3H₂O. The theoretical total metal contents of both Ru and Cu in the bimetallic Ru-Cu/SiO₂ catalyst were controlled as 2.5wt% (the total metal content in the catalyst was 5wt%).

Characterization

The XRD patterns of different catalysts were obtained on a PANalytical X'pert diffractometer operated at 40 kV and 40 mA, using nickel-filtered Cu K_{α} radiation. Before the tests, the samples were reduced by hydrogen at 673 K for 2 h (the same pretreat conditions as we used in HDO tests).

Hydrogen-temperature programmed reduction (H₂-TPR) tests of catalysts were conducted by a Micromeritics AutoChem II 2920 Automated Catalyst Characterization System. Before the tests, the samples were pretreated in Ar flow at 573 K for 0.5 h to remove adsorbed water and cooled to 323 K. At this moment, the gas was switched to 10vol% H₂ in Ar. After the stabilization of baseline, the samples were heated from 323 K to 1073 K at a rate of 10 K min⁻¹. The amount of H₂ consumption was monitored by a thermal conductivity detector (TCD). Before the TCD, the gas passed through a cold trap to remove the water generated during the test.

The high-resolution transmission electron microscopy (HRTEM) images of the HDO catalysts were collected by a JEM-2100F field emission electronic microscope. Prior to characterization, the catalysts were pretreated in hydrogen flow at 673 K for 2 h. The element distribution of the Ru-Cu/SiO₂ catalyst was analyzed by a TEM (JEOL JEM-2100F) which was equipped with energy dispersive X-ray spectroscopy (EDX) instrument. Before microscopy examination, the sample was first suspended in ethanol by ultrasonic method then loaded on a holey carbon film supported by a nickel TEM grid.

In-situ diffuse reflectance infrared Fourier transform spectroscopy (*In-situ* DRIFTS) of the catalysts were acquired at a spectral resolution of 4 cm⁻¹ and an accumulation of 128 scans by a BRUKER Equinox 70 spectrometer which was equipped with a MCT detector. Before each measurement, the catalyst was reduced *in-situ* by H₂ at 673 K for 1 h, then purged with He for 0.5 h. After the sample was cooled down to room temperature, the spectrum was acquired and used as the background. Subsequently, 5vol% CO/He was introduced into the cell until the steady state was reached. The excess CO was removed from the system by purging with He. Finally, the spectra were acquired and subtracted with the background.

In-situ XPS analysis was carried out by a ThermoFisher ESCALAB 250Xi spectrometer at 15 kV, 10.8 mA employing Al K_{α} X-ray ($h = 1486.6$ eV, analysis chamber base pressure > 3 × 10⁻⁸ Pa). Prior to analysis, the catalysts were pretreated with hydrogen flow at 673 K for 2 h.

Activity tests

The alcoholysis of PET waste was carried out in a 100 mL stainless steel batch reactor (Parr 4848) under nitrogen atmosphere. For each test, 1 g PET waste and 40 mL alcohol (such as methanol, ethanol and butanol) were used. After purging the reactor with nitrogen for three times, the mixture was stirred at 413-473 K for 3.5 h, then quenched to room temperature with cool water. Subsequently, an excess amount of methanol was added into the reaction system. According to the saturated solutions of terephthalate products at room temperature, the amount of methanol used in this work was more than enough to dissolve the terephthalates from the alcoholysis of PET waste even when they were produced at 100% yield. The residual PET is unsolvable in methanol. Therefore, it was easily separated from the alcoholysis product by filtration, dried at 343 K overnight and weighted to

calculate the conversion of PET. The terephthalates generated during the alcoholysis reactions were solved in methanol and quantitatively analyzed by an Agilent 7890A GC. The PET conversions and the terephthalate yields during alcoholysis tests were calculated according following equations.

Conversion of PET waste (%) = (Initial weight of PET waste - the weight of residual PET waste)/(Initial weight of PET waste) × 100%

Yield of terephthalate (%) = (Mole of terephthalate generated during the alcoholysis test)/(Theoretical mole of terephthalate which should be produced from the complete conversion of the PET waste) × 100%

The solvent-free hydrogenation of DMT was carried out in a 100 mL stainless steel batch reactor (Parr 4848). For each test, 30 g DMT and 1 g catalyst was used. After purging the reactor and filling it with hydrogen, the mixture of DMT and catalyst was heated to 353-433 K and vigorously stirred at that temperature for certain time. During the reaction, hydrogen was added from time to time to keep the system pressure at 5 MPa. After the test, the reactor was quenched to room temperature with cool water. The unreacted hydrogen was released. The liquid product was separated with catalyst by filtration, diluted and analyzed by an Agilent 7890A GC. The DMT conversions and yields of DMCD during hydrogenation tests were calculated according following equations.

Conversion of DMT (%) = (Initial mole of DMT in the feedstock - mole of unreacted DMT in the product)/(Initial mole of DMT in the feedstock) × 100%

Yield of DMCD (%) = (Mole of DMCD in the product/Mole of DMT in the feedstock) × 100%

The solvent-free HDO of DMCD was carried out in a 316 L stainless steel fixed-bed tubular reactor which has been described in our previous work.¹⁴ Prior to reaction, the catalysts (1.8 g) were *in-situ* reduced by H₂ flow at 673 K for 2 h. After cooling down the reactor to reaction temperature and increasing the system pressure to set values, DMCD was pumped into the reactor (at a rate of 0.04 mL min⁻¹) with hydrogen (at a flow rate of 120 mL min⁻¹). The products from the outlet of the reactor become two phases in a gas-liquid separator. The gaseous products passed through the back-pressure regulator and were analyzed online by an Agilent 7890A GC. The liquid phase products were withdrawn periodically from the gas-liquid separator and analyzed by another Agilent 7890A GC. The conversion of DMCD and the yields of C₇-C₈ aromatics and cycloalkanes during HDO tests were calculated according to following equations.

Conversion of DMCD (%) = (Mole of DMCD fed into the reactor - mol of unreacted DMCD in the HDO product)/(Mole of DMCD fed into the reactor) × 100%

Yield of C₇-C₈ aromatics (%) = (Mole of C₇-C₈ aromatics in the HDO product/Mole of DMCD fed into the reactor) × 100%

Yield of C₇-C₈ cycloalkanes (%) = (Mole of C₇-C₈ cycloalkanes in the HDO product/Mole of DMCD fed into the reactor) × 100%

Results and discussion

Characterization.

The crystalline phases of HDO catalysts were characterized by XRD. From Figure 1, we can only observe the peaks of metallic Ru and Cu in the XRD patterns of Ru/SiO₂ and Cu/SiO₂ catalysts. No peaks of Ru (or Cu) oxides were observed. These results mean that the Ru and Cu species can be reduced to metallic state after being pretreated in hydrogen flow at 673 K for 2 h. Different with those of the Ru/SiO₂ and Cu/SiO₂ catalysts, the XRD pattern of the bimetallic Ru-Cu/SiO₂ catalyst only has one peak at 44.1°. The intensity of this peak is evidently lower than the peak of Ru (101) in the XRD patterns of Ru/SiO₂ catalyst.

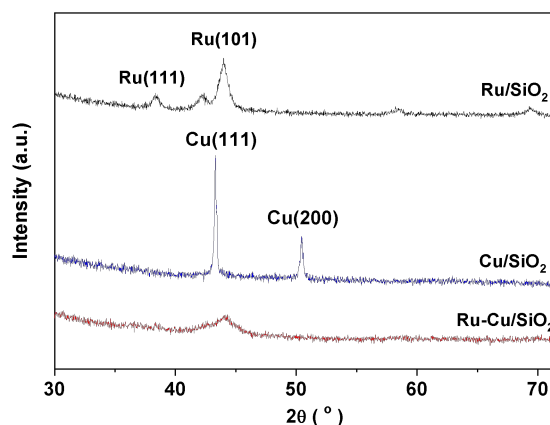


Figure 1. XRD patterns of the Ru/SiO₂, Cu/SiO₂ and Ru-Cu/SiO₂ catalysts.

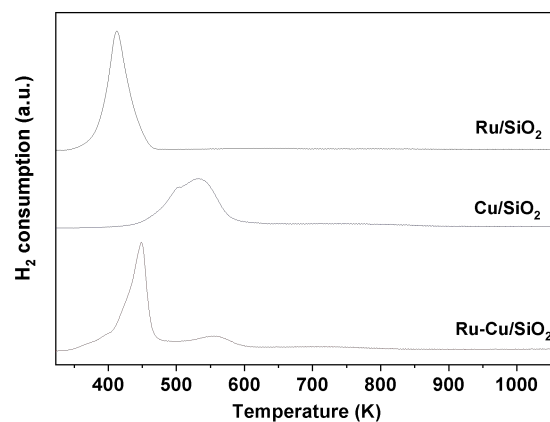


Figure 2. H₂-TPR profiles of the Ru/SiO₂, Cu/SiO₂ and Ru-Cu/SiO₂ catalysts.

The redox properties of the Ru/SiO₂, Cu/SiO₂ and Ru-Cu/SiO₂ catalysts were investigated as well. From Figure 2, we can see that the H₂-TPR profile of Ru/SiO₂ has a peak at 413 K. According to literature,¹⁵ this peak can be assigned to the reduction of RuO₂ to metallic Ru. The H₂-TPR profile of Cu/SiO₂ catalyst demonstrated an unresolved peak range between 450 K and 580 K. According to previous report,¹⁶ the peak centred at 502 K can be attributed to the reduction of CuO to Cu₂O, while the peak centred at 533 K can be explained by the further reduction of Cu₂O to metallic Cu. Different with the Ru/SiO₂ and Cu/SiO₂ catalysts, the H₂-TPR profile of the Ru-Cu/SiO₂ catalyst exhibited a main peak at 448 K and a small shoulder peak at 555 K. Compared with the Ru/SiO₂ catalyst, the main reduction peak in the H₂-TPR profile of Ru-Cu/SiO₂

catalyst shifted to a higher temperature. From this result, we can see that there is some strong interaction between the Ru and Cu species in the Ru-Cu/SiO₂ catalyst. Moreover, it was also noticed that the reduction peak of Cu species at 555 K is very weak and evidently lower than what it should be (as compared to that for the Cu/SiO₂ catalyst). This phenomenon could be rationalized because the hydrogen spillover effect of Ru species promoted the reduction of CuO_x species.¹⁷ As the result, some reduction peak CuO_x species was shifted to lower temperature and involved in the main reduction peak in the H₂-TPR profile of Ru-Cu/SiO₂ catalyst.

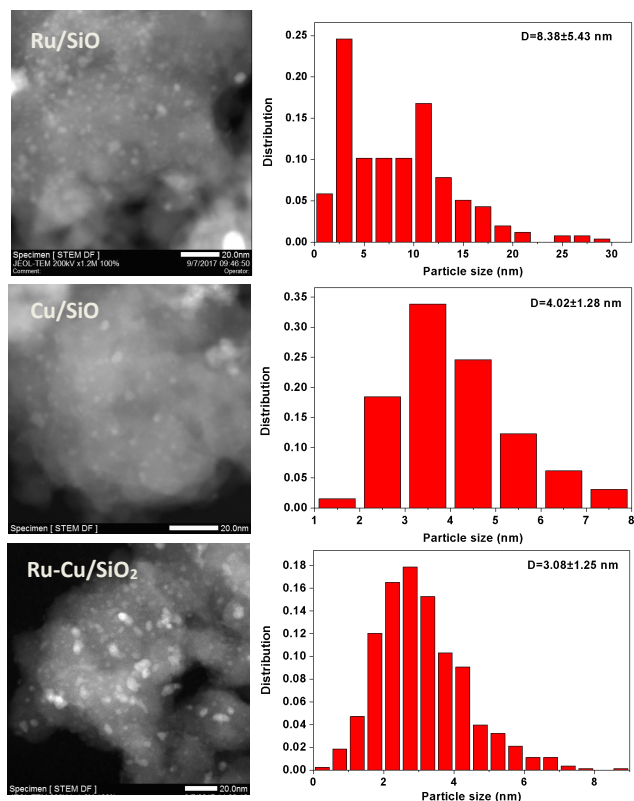


Figure 3. TEM images of the Ru/SiO₂, Cu/SiO₂ and Ru-Cu/SiO₂ catalysts.

Figure 3 shows the TEM images of the Ru/SiO₂, Cu/SiO₂ and Ru-Cu/SiO₂ catalysts. According to the statistical results, the average diameter of metal particles on the surface of the Ru-Cu/SiO₂ catalyst is evidently lower than those over the Ru/SiO₂ and Cu/SiO₂ catalysts, which is in line with the XRD results.

According to Figure 4a, the lattice spacing of the metallic particles on the Ru-Cu/SiO₂ catalyst was estimated as 0.20 nm. This lattice spacing is larger than that of Cu(200) (0.18 nm)¹⁸ but smaller than the lattice spacing of the Ru(101) (0.21 nm).¹⁹ Based on this result, we think that Ru-Cu alloy was formed on the surface of Ru-Cu/SiO₂ catalyst. To further verify this hypothesis, we also characterized the Ru-Cu/SiO₂ catalyst by X-ray energy dispersive spectroscopy (X-EDS). From the X-EDS spectra (see Figure 4c) of some points which were randomly chosen in the area shown in Figure 4b, both Ru and Cu species were observed simultaneously. This result further confirms the formation of Ru-Cu alloy on the surface of Ru-Cu/SiO₂ catalyst.

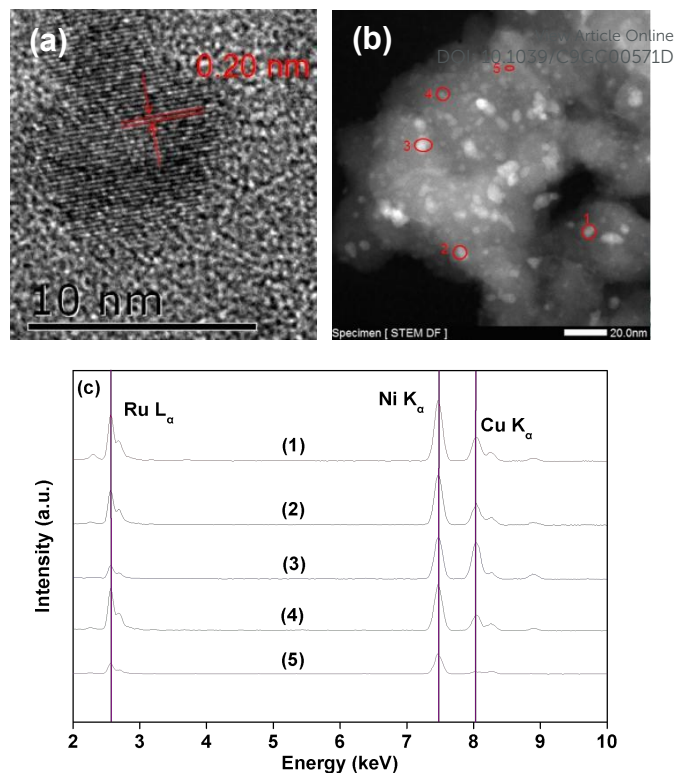


Figure 4. HRTEM image (a) and X-EDS spectra (b, c) of the Ru-Cu/SiO₂ catalyst.

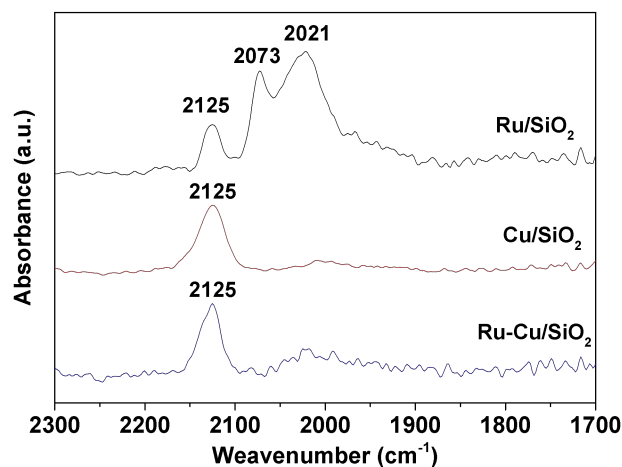


Figure 5. CO DRIFTS of the Ru/SiO₂, Cu/SiO₂ and Ru-Cu/SiO₂ catalysts.

From Figure 5, we can see that the CO DRIFTS of Ru/SiO₂ catalyst has three peaks at 2125 cm⁻¹, 2073 cm⁻¹ and 2021 cm⁻¹. According to literature,²⁰ the peak at 2021 cm⁻¹ can be assigned to the CO which is linearly adsorbed on Ru⁰, while the two bands at 2073 cm⁻¹ and 2125 cm⁻¹ can be attributed to the CO which is linearly adsorbed on Ru^{δ+} sites. The CO DRIFTS of Cu/SiO₂ catalyst only has one peak at 2125 cm⁻¹ which should be assigned to the CO which is linearly adsorbed on Cu⁰. Similar to that of Cu/SiO₂, the CO DRIFTS of Ru-Cu/SiO₂ catalyst also has a unique peak at 2125 cm⁻¹. As what has been suggested in literature,²¹ this phenomenon may be explained by the enrichment of Cu on the surface of Ru-Cu alloy particles formed on the Ru-Cu/SiO₂ catalyst.

Figure 6 shows the XPS spectra of the Ru/SiO₂, Cu/SiO₂ and Ru-Cu/SiO₂ catalysts. From the binding energies of Ru 3d and Cu 2p in these catalysts, we can see that the Ru and Cu species in the catalysts exist as metallic states. This is consistent with the XRD results. Compared with the monometallic Ru/SiO₂ and Cu/SiO₂ catalysts, the binding energies of both Ru 3d and Cu 2p in the bimetallic Ru-Cu/SiO₂ catalyst shift to a lower values. This result can be considered as another evidence for the strong interaction (or electrons transfer) between the Ru and Cu species in the bimetallic Ru-Cu/SiO₂ catalyst.²²

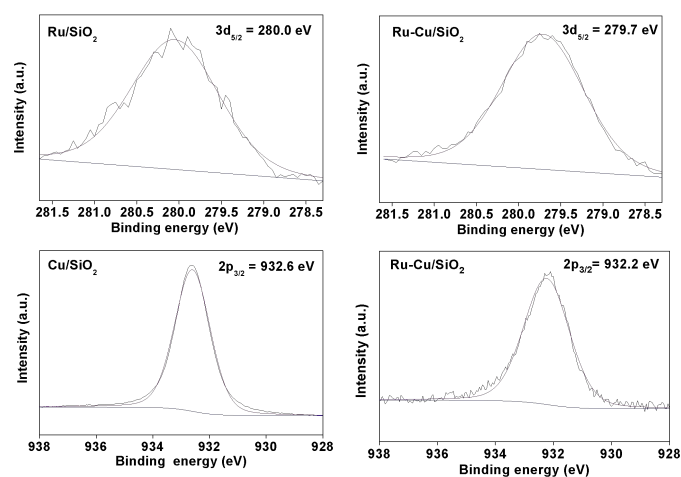


Figure 6. Ru 3d and Cu 2p XPS spectra of the Ru/SiO₂, Cu/SiO₂ and Ru-Cu/SiO₂ catalysts.

Activity test

Alcoholysis of PET waste. First of all, we studied the depolymerisation of PET waste by alcoholysis with a series of alcohols (see Figure 7). Among them, methanol exhibited the highest reactivity for the alcoholysis of PET waste. This is consistent with what has been reported by literature.⁸ After the alcoholysis reaction was carried out in methanol at 453 K for 3.5 h, PET waste was completely converted in the absence of any catalyst. High yield (90.1%) of DMT was achieved.

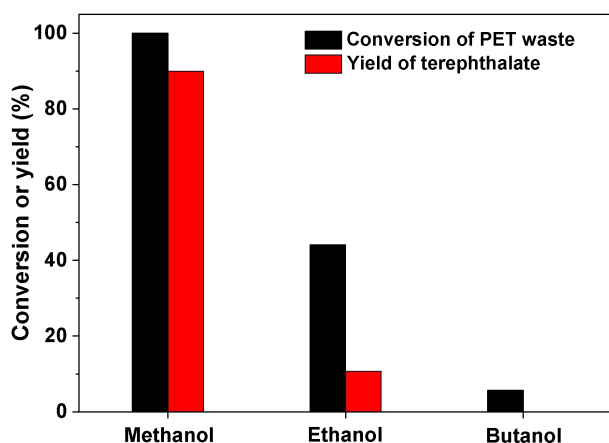
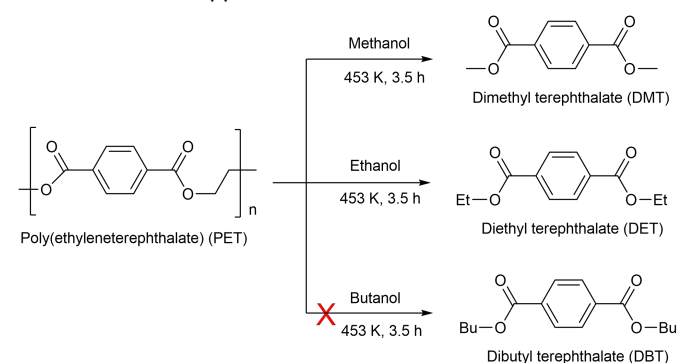


Figure 7. Conversions of PET waste and the yields of terephthalates from the alcoholysis of PET waste in the absence of catalyst. Reaction conditions: 453 K, 3.5 h; 1 g PET waste and 40 mL alcohol were used in each test.

Besides methanol, ethanol was also found to be effective for the alcoholysis of PET waste. However, its reactivity is evidently lower than that of methanol. In contrast, the butanol is inactive for the alcoholysis of PET waste under the investigated conditions (see Figure S1 in supporting information). The reaction pathways for the generation of DMT and diethyl terephthalate (DET) from the alcoholysis of PET were proposed in Scheme 2. Taking into consideration the lower price and higher reactivity of methanol than ethanol and butanol, we think that it is a good choice for the alcoholysis of PET waste in real application.



Scheme 2. Reaction pathways for the alcoholysis of PET waste with different alcohols at 453 K.

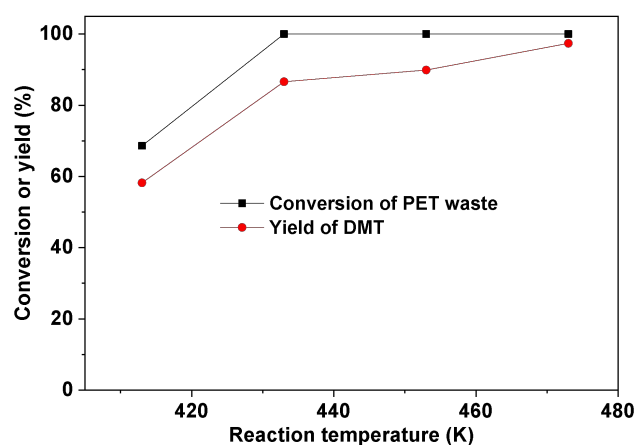


Figure 8. Conversion of PET waste and the DMT yield from the methanolysis of PET waste as the function of reaction temperature. Reaction conditions: 3.5 h; 1 g PET waste and 40 mL methanol were used in each test.

The effects of reaction conditions (such as reaction temperature, mass of substrate and reaction time) on the methanolysis of PET waste were investigated as well. From Figure 8, we can see that methanol is very reactive for the alcoholysis of PET waste. High PET conversion (100%) and DMT yield (86.5%) were achieved even at 433 K. After we raised reaction temperature to 473 K, the PET waste was almost totally converted to DMT (in a yield of 97.3%) after 3.5 h. With the increase of substrate concentration in the reaction system, the PET conversion and DMT yield decreased (see Figure 9). However, this problem can be solved by further increase reaction time (see Figure 10).

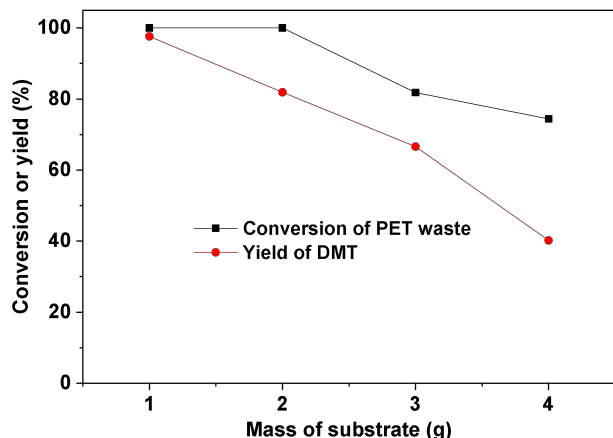


Figure 9. Conversion of PET waste and the DMT yield from the methanolysis of PET waste as the function of substrate mass. Reaction conditions: 473 K, 3.5 h; 40 mL methanol were used in each test.

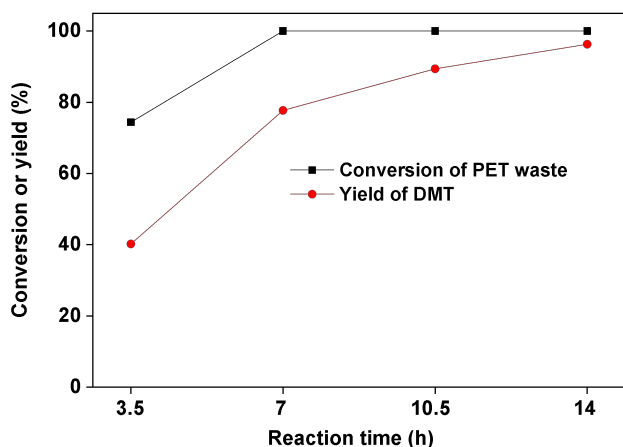


Figure 10. Conversion of PET waste and the DMT yield from the methanolysis of PET waste as the function of reaction temperature. Reaction conditions: 473 K; 4 g PET waste and 40 mL methanol were used in each test.

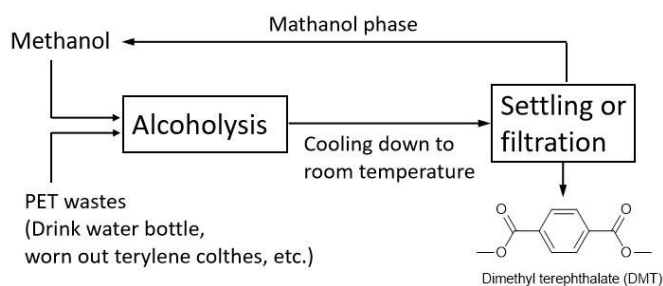


Figure 11. Block flow diagram for the production of DMT with PET waste and methanol.

Due to its low solubility in methanol, most of the DMT generated during the alcoholysis test automatically separated from methanol when the reaction system was cooled down to room temperature (see Figure S2 in supporting information). In real application, this is advantageous because the energy consumption can be decreased if we can separate methanol

and DMT by settling (or filtration) instead of distillation. The methanol phase which contains small amount DMT can be recycled and reused for the alcoholysis of PET waste (see Figure 11).

Solvent-free hydrogenation of DMT. As we mentioned earlier, the DMT obtained from the alcoholysis of PET waste exists as a solid at room temperature. To increase its fluidity, we hydrogenated it before the HDO test. The hydrogenation of DMT was carried over a series of activated carbon loaded noble metal catalysts under solvent-free conditions. Based on the analysis of hydrogenation product by GC-MS, DMCD was identified as the major product from the solvent-free hydrogenation of DMT (see Figure S3 in supporting information). Among the investigated catalysts, Pt/C exhibited the highest activity for the hydrogenation of DMT to DMCD (see Figure 12). Over the Pt/C catalyst, high DMT conversion (73.1%) and good DMCD yield (71.1%) were achieved after the reaction was carried out at 373 K for 7 h. The activities of investigated catalysts decrease in the order of Pt/C > Ru/C > Pd/C. This sequence is consistent with the activity sequence of these catalysts for hydrogenation of other aromatic compounds such as *p*-xylene (see Figure S4 in supporting information). Based on these results, we can attribute the higher DMT conversion and DMCD yield over the Pt/C to the high activity of this catalyst for the hydrogenation of benzene ring.

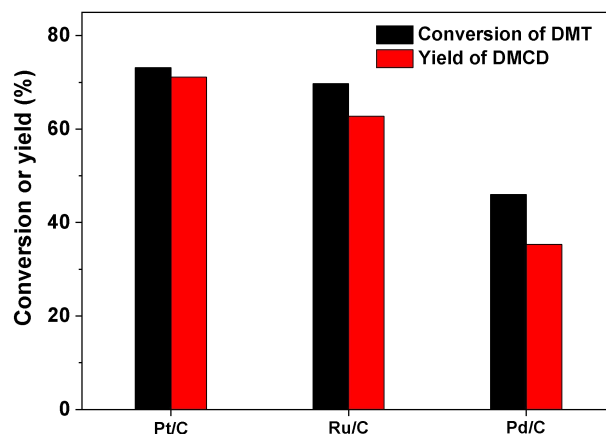


Figure 12. Conversions of DMT and the yields of DMCD over different noble metal catalysts. Reaction conditions: 373 K, 5 MPa H₂, 7 h; 30 g DMT and 1 g catalyst were used in each test.

The effects of reaction conditions (such as reaction temperature, catalyst dosage and reaction time) over the catalytic performance of Pt/C were investigated (see Figures 13-15). Under the optimized conditions (413 K, 1.0 g catalyst and 10 h), DMT was completely converted and high yield (99.2 %) of DMCD was achieved over the Pt/C catalyst (see Figure 15). The DMCD obtained from the hydrogenation of DMT exists as a liquid at room temperature (see Figure S5 in supporting information). Therefore, it can be directly used for the subsequent HDO process in the absence of solvent.

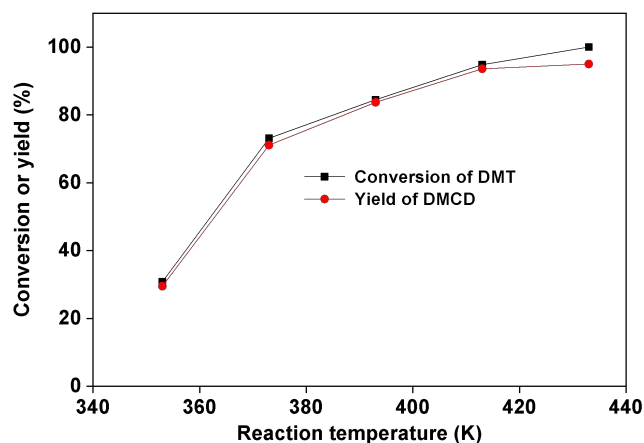


Figure 13. Conversion of DMT and the yield of DMCD over the Pt/C catalyst as the function of reaction temperature. Reaction conditions: 5 MPa H₂, 7 h; 30 g DMT and 1 g Pt/C catalyst were used in each test.

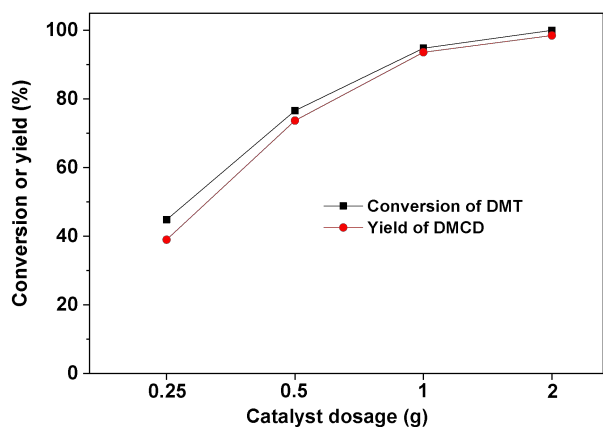


Figure 14. Conversion of DMT and the yield of DMCD over the Pt/C as the function of catalyst dosage. Reaction conditions: 413 K, 5 MPa H₂, 7 h; 30 g DMT was used in each test.

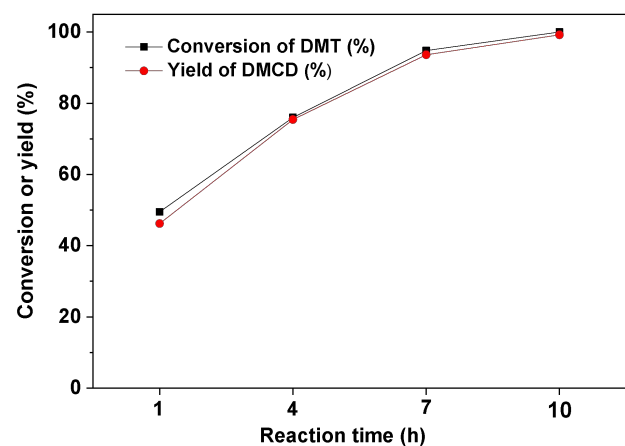


Figure 15. Conversion of DMT and the yield of DMCD over the Pt/C catalyst as the function of reaction time. Reaction conditions: 413 K, 5 MPa H₂; 30 g DMT and 1 g Pt/C catalyst were used in each test.

Solvent-free HDO of DMCD. As the final aim of this work, we studied the solvent-free HDO of DMCD over the Ru/SiO₂,

Cu/SiO₂ and bimetallic Ru-Cu/SiO₂ catalysts. The activity tests were carried out at 643 K and 6 MPa H₂. From the analysis of gas phase and liquid phase products, it was found that DMCD was completely converted over the Ru/SiO₂ catalyst. Methane was identified as the major product (see Table S2 in supporting information). This result can be explained by the high methanation activity of Ru catalyst. In contrast, DMCD was only partially hydrodeoxygenated over the Cu/SiO₂ catalyst (see Figure 16 and the Figure S6 in supporting information). Low total yield (32.1%) of C₇-C₈ hydrocarbons was obtained under the investigated conditions. Compared with the Ru/SiO₂ and Cu/SiO₂, the bimetallic Ru-Cu/SiO₂ catalyst exhibited evident advantage in the HDO of DMCD. Over it, DMCD was completely converted under the investigated conditions. High total yield of C₇-C₈ cycloalkanes and aromatics (93.9%) was achieved. Based on the characterization results, the excellent performance of Ru-Cu/SiO₂ catalyst can be explained by the formation of smaller Ru-Cu alloy which has higher efficiency for hydrodeoxygenation than Cu and lower methanation activity than Ru. As potential applications, the C₇-C₈ hydrocarbons as obtained can be either used as gasoline (the octane numbers of the C₇-C₈ hydrocarbons were listed in Table S3 in supporting information) to reduce the dependence of our society on fossil energy or blended into bio-jet fuels to improve their densities (or heat values) and sealabilities. The methane which was obtained as by-product from the HDO of DMCD can be oxidized to methanol which is used in the alcoholysis step.²³

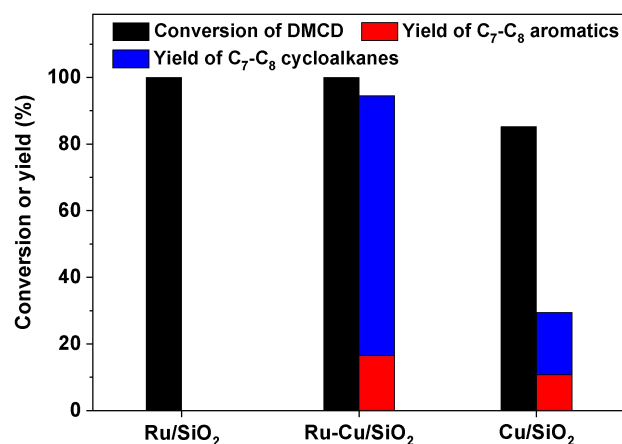
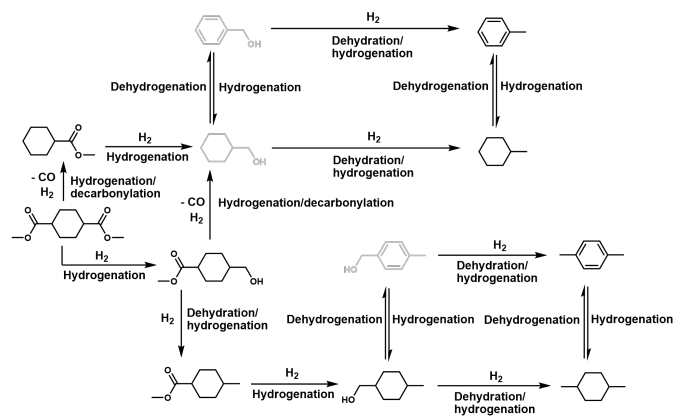


Figure 16. Conversions of DMCD and the yields of different hydrocarbons over the Ru/SiO₂, Cu/SiO₂ and Ru-Cu/SiO₂ catalysts. Reaction conditions: 643 K, 6 MPa H₂; 1.8 g catalyst, DMCD feedspeed: 0.04 mL min⁻¹, H₂ flow rate: 120 mL min⁻¹.

According to the literature about the HDO of esters²⁴ and the intermediates which were identified in the GC-MS chromatogram of HDO product at a space velocity which was four times of the one used in the HDO tests (see Figure S7-S12 in supporting information), the reaction pathways for the production of C₇-C₈ cycloalkanes and aromatics from the HDO of DMCD was proposed (see Scheme 3). From Scheme 3, we can see that the C₈ cycloalkanes in the HDO product were generated by the hydrogenation of ester groups of DMCD followed by dehydration and hydrogenation, while the C₈ aromatics were generated by the hydrogenation of ester

groups of DMCD followed by dehydrogenation, dehydration and dehydrogenation. Different with C₈ hydrocarbons, the reaction pathways for the generation of C₇ cycloalkanes and aromatics also involves an additional hydrogenation/decarbonylation step (this has been proved by the presence of CO in the gas phase product (see Table S2 in supporting information)). As the result, one carbon atom will be lost from the carbon chain of DMCD.



Scheme 3. Reaction pathways for the generation of C₇-C₈ cycloalkanes and aromatics from the solvent-free HDO of DMCD.

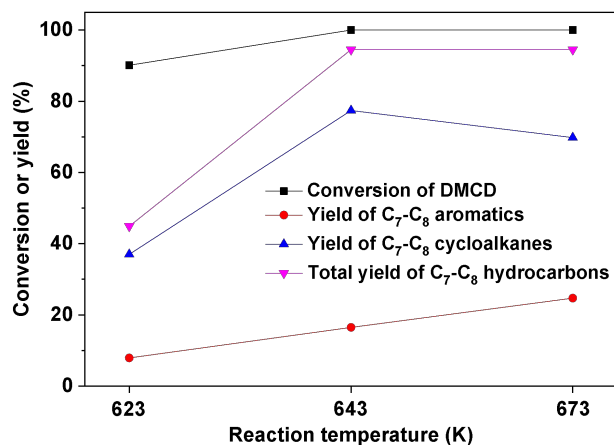


Figure 17. Conversion of DMCD and the yields of different hydrocarbons over the Ru-Cu/SiO₂ catalyst as the function of reaction temperature. Reaction conditions: 6 MPa; 1.8 g Ru-Cu/SiO₂ catalyst, DMCD feedspeed: 0.04 mL min⁻¹, H₂ flow rate: 120 mL min⁻¹.

The effects of reaction temperature and system pressure on the yields of C₇-C₈ cycloalkanes and aromatics over the bimetallic Ru-Cu/SiO₂ catalyst were investigated. From the results illustrated in Figure 17, we can see that the conversion of DMCD and the total yield of C₇-C₈ hydrocarbons over the Ru-Cu/SiO₂ catalyst increased with reaction temperature, reached the maximum at 643 K and stabilized with the further increase of reaction temperature to 673 K. Analogous relationship was found between the system pressure and the conversion of DMCD or the total yield of C₇-C₈ hydrocarbons over the Ru-Cu/SiO₂ catalyst (see Figure 18). Meanwhile, it was also noticed that higher reaction temperature and lower system pressure are favourable for the production of C₇-C₈

aromatics from the HDO of DMCD. This can be comprehended from the viewpoints of thermodynamics (because dehydrogenation is an endothermic reaction) and reaction equilibrium. Subsequently, we also explored the catalyst dosage on the performance of Ru-Cu/SiO₂. From Figure 19, it was noticed that the DMCD conversion, the total yield of cyclic hydrocarbons and the yield of C₇-C₈ aromatics over Ru-Cu/SiO₂ increased with the catalyst dosage and reached the maximum when 1.8 g catalyst was used for the test. In contrast, a volcanic shape relationship was observed between the catalyst dosage and the yield of C₇-C₈ cycloalkanes over Ru-Cu/SiO₂ catalyst. These results further confirm that the C₇-C₈ aromatics are generated from the dehydrogenation of C₇-C₈ cycloalkanes.

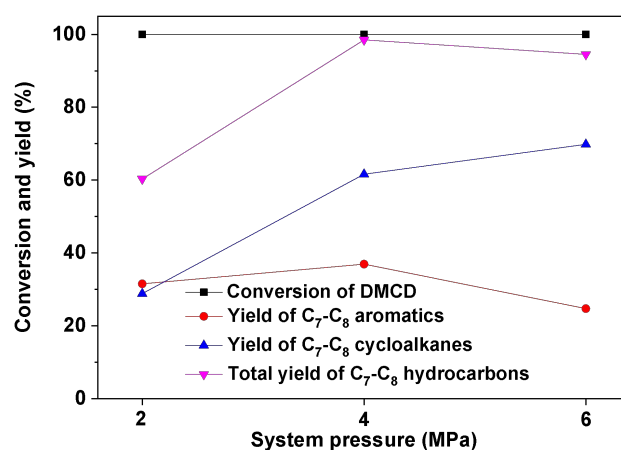


Figure 18. Conversion of DMCD and the yields of different hydrocarbons over the Ru-Cu/SiO₂ catalyst as the function of system pressure. Reaction conditions: 673 K; 1.8 g Ru-Cu/SiO₂ catalyst, DMCD feedspeed: 0.04 mL min⁻¹, H₂ flow rate: 120 mL min⁻¹.

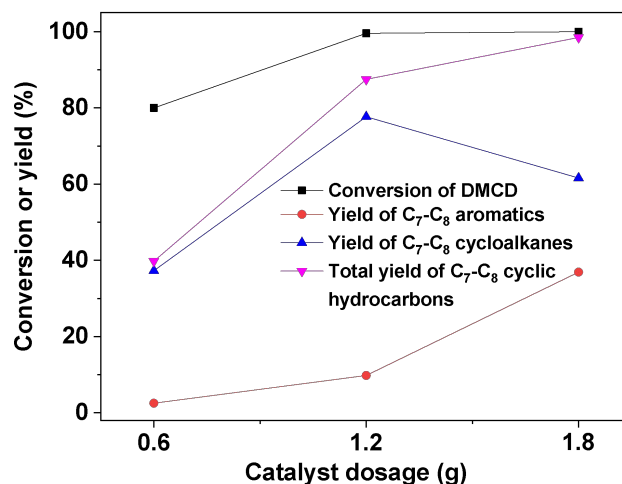


Figure 19. Conversion of DMCD and the yields of different hydrocarbons over the Ru-Cu/SiO₂ as the function of catalyst dosage. Reaction conditions: 4 MPa, 673 K; 1.8 g Ru-Cu/SiO₂ catalyst, DMCD feedspeed: 0.04 mL min⁻¹, H₂ flow rate: 120 mL min⁻¹.

In real application, the production of aromatics from the HDO of DMCD is advantageous due to following two reasons. 1) As we can see from Table S3 in supporting information, the C₇-C₈ aromatics as obtained have higher octane numbers and

densities than those of the C₇-C₈ cycloalkanes. Moreover, the presence of aromatic hydrocarbons in the jet fuel is also necessary to ensure the shrinkage of aged elastomer seals and prevent the leakage of fuel. For safety reason, there must be 8-25% aromatic hydrocarbons in the current jet fuels.²⁵ 2) From the point view of stoichiometry, the production of C₇-C₈ aromatics from the HDO of DMCD needs less hydrogen than the one which is need for the production of C₇-C₈ cycloalkanes. Taking into consideration of the total yield of C₇-C₈ hydrocarbons, octane numbers and densities of specific hydrocarbon products and the influence system pressure or reaction temperature on facility cost and energy consumption, we think that 673 K, 4 MPa and 1.8 g catalyst are the optimized reaction conditions for the HDO of DMCD over the Ru-Cu/SiO₂ catalyst.

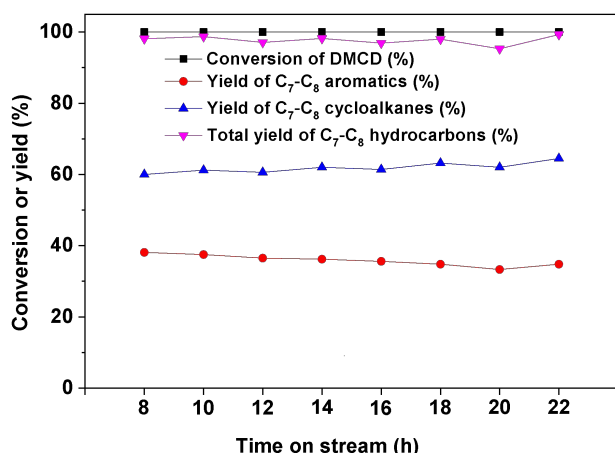


Figure 20. Conversion of DMCD and the yields of different hydrocarbons over the Ru-Cu/SiO₂ catalyst as the function of time on stream. Reaction conditions: 673 K, 4 MPa H₂; 1.8 g Ru-Cu/SiO₂ catalyst, DMCD flow rate: 0.04 mL min⁻¹, H₂ flow rate: 120 mL min⁻¹.

To fulfil the need of real application, we also checked the stability of the Ru-Cu/SiO₂ catalyst for the solvent-free HDO of DMCD under the optimized conditions (673 K and 4 MPa H₂). From Figure 20 and Figure S13 in supporting information, no evident deactivation of the Ru-Cu/SiO₂ catalyst was observed during the 22 h continuous tests. This result indicates that the Ru-Cu/SiO₂ catalyst is stable under the investigated conditions. As we know, HDO is an important step in many reported routes for bio-jet fuel production. To decrease the investment of facility, we also explored the solvent-free simultaneous HDO of DMCD and some representative bio-jet fuel precursors. Methyl laurate and 5,5'-(butane-1,1-diyl)bis(2-methylfuran) are two representative bio-jet fuel precursors which can be produced by the transesterification of lauric oils²⁶ or the hydroxylalkylation/alkylation of lignocellulose derived 2-methylfuran and butanal.²⁷ In this work, we investigated the solvent-free HDO of the mixtures which were prepared with the same mass of DMCD and methyl laurate (or 5,5'-(butane-1,1-diyl)bis(2-methylfuran)). Under the optimized reaction conditions (673 K and 4 MPa H₂), all of the oxygenates in the feedstocks were completely hydrodeoxygenated over the Ru-Cu/SiO₂ catalyst. High yield of jet fuel range chain alkanes,

cycloalkanes and aromatics were obtained at the same time (see Table 1). In the future application, it is possible to use biomass and PET waste simultaneously to produce jet fuel with proper contents of cycloalkanes and aromatics.

Table 1. Conversions of feedstocks, the yields of different hydrocarbons from the solvent-free simultaneous HDO of DMCD and biomass derived jet fuel precursors. Reaction conditions: 673 K, 4 MPa H₂; 1.8 g Ru-Cu/SiO₂ catalyst, feedspeed of liquid reactants: 0.04 mL min⁻¹, H₂ flow rate: 120 mL min⁻¹.

Conversion or yield ^a	Feedstock 1 ^b	Feedstock 2 ^c
Conversion of DMCD (%)	100	100
Conversion of methyl laurate (%)	100	—
Conversion of 5,5'-(butane-1,1-diyl)bis(2-methylfuran) (%)	—	100
Yield of C ₇ -C ₈ aromatics (%)	33.4	32.1
Yield of C ₇ -C ₈ cycloalkanes (%)	64.9	65.7
Total yield of C ₇ -C ₈ cyclic hydrocarbons (%)	98.3	97.8
Yield of C ₈ -C ₁₆ jet fuel chain alkanes (%)	99.8	81.8

^a The conversions of feedstocks and yields of different products were calculated according to the method described in supporting information.

^b Mixture of DMCD and methyl laurate at the mass ratio of 1:1. ^c Mixture of DMCD and 5,5'-(butane-1,1-diyl)bis(2-methylfuran) at the mass ratio of 1:1.

Conclusions

Gasoline and jet fuel range C₇-C₈ cycloalkanes and aromatics were produced at high overall yield (95%) by the alcoholysis of PET waste, followed by the solvent-free hydrogenation and HDO. Methanol was found to be highly reactive for the alcoholysis of PET waste. In the absence of catalyst, 97.3% yield of DMT was achieved from the methanolysis of PET waste after the reaction was carried out at 473 K for 3.5 h. The DMT as obtained can be automatically separated from methanol at room temperature and liquefied to DMCD by the solvent-free hydrogenation over Pt/C catalyst. Finally, the DMCD was further hydrodeoxygenated to gasoline and jet fuel range C₇-C₈ cycloalkanes and aromatics over bimetallic Ru-Cu/SiO₂ catalyst. Under the optimized conditions, 98.4% total yield of C₇-C₈ cycloalkanes and aromatics was achieved. The C₇-C₈ cyclic hydrocarbons as obtained can be blended with conventional bio-jet fuel to improve their densities (or volumetric heat values) and sealabilities. In future application, it is also possible to combine the hydrodeoxygenation of DMCD with those of biomass derived jet fuel precursors to produce jet fuel with proper contents of cycloalkanes and aromatics. This work offered a feasible method for the utilization of PET wastes to make the most demanded transportation liquid fuels.

Conflicts of interest

There are no conflicts to declare.

Acknowledgements

This work was supported by the National Natural Science Foundation of China (no. 21690082; 21776273; 21721004), DNL Cooperation Fund, CAS (DNL180301), the Strategic Priority Research Program of the Chinese Academy of Sciences

(XDB17020100, XDA 21060200), the National Key Projects for Fundamental Research and Development of China (2016YFA0202801), Dalian Science Foundation for Distinguished Young Scholars (no. 2015R005).

Notes and references

- G. W. Huber, S. Iborra and A. Corma, *Chem. Rev. (Washington, DC, U. S.)*, 2006, **106**, 4044-4098; S. Shylesh, A. A. Gokhale, C. R. Ho and A. T. Bell, *Acc. Chem. Res.*, 2017, **50**, 2589-2597; G. W. Huber, J. N. Chhedha, C. J. Barrett and J. A. Dumesic, *Science*, 2005, **308**, 1446-1450; Y. Roman-Leshkov, C. J. Barrett, Z. Y. Liu and J. A. Dumesic, *Nature*, 2007, **447**, 982-985; N. Yan, Y. Yuan, R. Dykeman, Y. Kou and P. J. Dyson, *Angew. Chem., Int. Ed.*, 2010, **49**, 5549-5553; Q. Xia, Z. Chen, Y. Shao, X. Gong, H. Wang, X. Liu, S. F. Parker, X. Han, S. Yang and Y. Wang, *Nat. Commun.*, 2016, **7**, 11162; Z. Cao, M. Dierks, M. T. Clough, I. B. Daltró de Castro and R. Rinaldi, *Joule*, 2018, **2**, 1118-1133.
- A. Corma, S. Iborra and A. Velty, *Chem. Rev. (Washington, DC, U. S.)*, 2007, **107**, 2411-2502; M. Besson, P. Gallezot and C. Pinel, *Chem. Rev. (Washington, DC, U. S.)*, 2014, **114**, 1827-1870; A. Wang and T. Zhang, *Acc. Chem. Res.*, 2013, **46**, 1377-1386; C. Li, X. Zhao, A. Wang, G. W. Huber and T. Zhang, *Chem. Rev. (Washington, DC, U. S.)*, 2015, **115**, 11559-11624; Y. L. Wang, W. P. Deng, B. J. Wang, Q. H. Zhang, X. Y. Wan, Z. C. Tang, Y. Wang, C. Zhu, Z. X. Cao, G. C. Wang and H. L. Wan, *Nat. Commun.*, 2013, **4**, 2141; T. Prasomsri, M. Shetty, K. Murugappan and Y. Roman-Leshkov, *Energy Environ. Sci.*, 2014, **7**, 2660-2669; F. Cao, T. J. Schwartz, D. J. McClelland, S. H. Krishna, J. A. Dumesic and G. W. Huber, *Energy Environ. Sci.*, 2015, **8**, 1808-1815; W. Deng, Y. Wang, S. Zhang, K. M. Gupta, M. J. Hülsey, H. Asakura, L. Liu, Y. Han, E. M. Karp, G. T. Beckham, P. J. Dyson, J. Jiang, T. Tanaka, Y. Wang and N. Yan, *Proc. Natl. Acad. Sci. U.S.A.*, 2018, **115**, 5093-5098; I. Scodeller, S. Mansouri, D. Morvan, E. Muller, K. de Oliveira Vigier, R. Wischert and F. Jérôme, *Angew. Chem., Int. Ed.*, 2018, **57**, 10510-10514.
- www.prnewswire.com/news-releases/plastics-market-worth-65438-billion-by-2020-grand-view-research-inc-511720541.html.
- U. T. Bornscheuer, *Science*, 2016, **351**, 1154-1155.
- S. Yoshida, K. Hiraga, T. Takehana, I. Taniguchi, H. Yamaji, Y. Maeda, K. Toyohara, K. Miyamoto, Y. Kimura and K. Oda, *Science*, 2016, **351**, 1196-1199.
- B. G. Mwanza and C. Mbohwa, *Procedia Manufacturing*, 2017, **8**, 649-656; Y.-B. Zhao, X.-D. Lv and H.-G. Ni, *Chemosphere*, 2018, **209**, 707-720.
- A. M. Al-Sabagh, F. Z. Yehia, G. Eshaq, A. M. Rabie and A. E. ElMetwally, *Egypt. J. Pet.*, 2016, **25**, 53-64; R. Koshti, L. Mehta and N. Samarth, *J. Polym. Environ.*, 2018, **26**, 3520-3529; B. Geyer, G. Lorenz and A. Kandelbauer, *Express Polym. Lett.*, 2016, **10**, 559-586; S. Jian, L. Dajiang, Y. R. P., C. A. G., I. N. G., S. Timo, C. J. R., S. B. A. and S. Seema, *ChemSusChem*, 2018, **11**, 781-792.
- D. Paszun and T. Szychaj, *Ind. Eng. Chem. Res.*, 1997, **36**, 1373-1383.
- S. Singh, S. Sharma, A. Umar, S. K. Mehta, M. S. Bhatti and S. K. Kansal, *J. Nanosci. Nanotechnol.*, 2018, **18**, 5804-5809.
- Q. Wang, X. Yao, Y. Geng, Q. Zhou, X. Lu and S. Zhang, *Green Chem.*, 2015, **17**, 2473-2479; Y. Geng, T. Dong, P. Fang, Q. Zhou, X. Lu and S. Zhang, *Polymer Degradation and Stability*, 2015, **117**, 30-36; Q. Wang, Y. Geng, X. Lu and S. Zhang, *ACS Sustainable Chem. Eng.*, 2015, **3**, 340-348.
- Y. Huang, Y. Ma, Y. Cheng, L. Wang and X. Li, *Ind. Eng. Chem. Res.*, 2014, **53**, 4604-4613.
- D. Hou, J. Xin, X. Lu, X. Guo, H. Dong, B. Ren and S. Zhang, *RSC Adv.*, 2016, **6**, 48737-48744; F. Zhang, J. Chen, P. Chen, Z. Sun and S. Xu, *AIChE J.*, 2012, **58**, 1853-1861.
- M. Jacquin, D. J. Jones, J. Rozière, S. Albertazzi, A. Vaccari, M. Lenarda, L. Storaro and R. Ganzerla, *Appl. Catal. A*, 2003, **251**, 131-141; A. B. Hungria, R. Raja, R. D. Adams, B. Captain, J. M. Thomas, P. A. Midgley, V. Golovko and B. F. G. Johnson, *Angew. Chem., Int. Ed.*, 2006, **45**, 4782-4785; H. Olcay, L. J. Xu, Y. Xu and G. W. Huber, *ChemCatChem*, 2010, **2**, 1420-1424; S. A. Kishore Kumar, M. John, S. M. Pai, Y. Niwate and B. L. Newalkar, *Fuel Process. Technol.*, 2014, **128**, 303-309; X. Guo, J. Xin, X. Lu, B. Ren and S. Zhang, *RSC Adv.*, 2015, **5**, 485-492; J. Escobar, M. C. Barrera, V. Santes and J. E. Terrazas, *Catal. Today*, 2017, **296**, 197-204.
- G. Li, N. Li, J. Yang, L. Li, A. Wang, X. Wang, Y. Cong and T. Zhang, *Green Chem.*, 2014, **16**, 594-599; J. Xu, N. Li, X. Yang, G. Li, A. Wang, Y. Cong, X. Wang and T. Zhang, *ACS Catal.*, 2017, **7**, 5880-5886.
- A. V. H. Soares, J. B. Salazar, D. D. Falcone, F. A. Vasconcellos, R. J. Davis and F. B. Passos, *J. Mol. Catal. A: Chem.*, 2016, **415**, 27-36.
- F. Lu, C. Yu, X. Meng, G. Chen and P. Zhao, *New J. Chem.*, 2017, **41**, 3280-3289.
- L. Hu, X. Liu, Q. Wang and Y. Zhou, *RSC Adv.*, 2017, **7**, 21507-21517.
- P. L. Hansen, J. B. Wagner, S. Helveg, J. R. Rostrup-Nielsen, B. S. Clausen and H. Topsøe, *Science*, 2002, **295**, 2053-2055.
- T. W. Hansen, J. B. Wagner, P. L. Hansen, S. Dahl, H. Topsøe and C. J. H. Jacobsen, *Science*, 2001, **294**, 1508-1510.
- S. Scirè, C. Crisafulli, R. Maggiore, S. Minicò and S. Galvagno, *Catal. Lett.*, 1998, **51**, 41-45; S. Eckle, H.-G. Anfang and R. J. Behm, *Appl. Catal., A*, 2011, **391**, 325-333; O. Dularent, X. Courtois, V. Perrichon and D. Bianchi, *J. Phys. Chem. B*, 2000, **104**, 6001-6011.
- C. Crisafulli, R. Maggiore, S. Scirè and S. Galvagno, *J. Chem. Soc., Faraday Trans.*, 1994, **90**, 2809-2813.
- T. Jiang, Y. Zhou, S. Liang, H. Liu and B. Han, *Green Chem.*, 2009, **11**, 1000-1006.
- P. Tomkins, M. Ranocchiaro and J. A. van Bokhoven, *Acc. Chem. Res.*, 2017, **50**, 418-425; V. L. Sushkevich, D. Palagin, M. Ranocchiaro and J. A. van Bokhoven, *Science*, 2017, **356**, 523-527; X. Cui, H. Li, Y. Wang, Y. Hu, L. Hua, H. Li, X. Han, Q. Liu, F. Yang, L. He, X. Chen, Q. Li, J. Xiao, D. Deng and X. Bao, *Chem*, 2018, **4**, 1902-1910.
- L. Chen, Y. Zhu, H. Zheng, C. Zhang and Y. Li, *Appl. Catal., A*, 2012, **411-412**, 95-104; B. X. Peng, X. G. Yuan, C. Zhao and J. A. Lercher, *J. Am. Chem. Soc.*, 2012, **134**, 9400-9405; L. M. He, C. Y. Wu, H. Y. Cheng, Y. C. Yu and F. Y. Zhao, *Catal. Sci. Technol.*, 2012, **2**, 1328-1331.
- Standard specification for aviation turbine fuel containing synthesized hydrocarbons, U. S. D. o. Defense Report ASTM D7566-14a, ASTM International, West Conshohocken, PA 19428-2959. United States, 2014.
- I. Ambat, V. Srivastava and M. Sillanpää, *Renewable and Sustainable Energy Reviews*, 2018, **90**, 356-369.
- A. Corma, O. de la Torre, M. Renz and N. Villandier, *Angew. Chem., Int. Ed.*, 2011, **50**, 2375-2378; G. Li, N. Li, J. Yang, A. Wang, X. Wang, Y. Cong and T. Zhang, *Bioresour. Technol.*, 2013, **134**, 66-72.